

## Miscut-angle dependence of perpendicular magnetic anisotropy in thin epitaxial CoPt<sub>3</sub> films grown on vicinal MgO

B. B. Maranville,<sup>a)</sup> A. L. Shapiro, and F. Hellman  
*Department of Physics, University of California at San Diego, La Jolla, California 92093*

D. M. Schaadt and E. T. Yu  
*Department of Electrical and Computer Engineering, University of California at San Diego, La Jolla, California 92093*

(Received 27 December 2001; accepted for publication 10 May 2002)

The effect of vicinal substrates on the growth-induced perpendicular magnetic anisotropy of epitaxial CoPt<sub>3</sub> films has been studied. A small (2°, 4°, or 10°) miscut angle of the vicinal substrate causes the crystallographic axes of the sample to be tilted along the miscut direction. The magnitude of the perpendicular anisotropy is unaffected by the presence of substrate steps produced by the miscut angle, while an additional, in-plane anisotropy develops with a larger miscut angle. Effects of the steps are seen in magnetic force microscopic images of domain wall pinning. © 2002 American Institute of Physics. [DOI: 10.1063/1.1491610]

CoPt<sub>3</sub> grown by vapor deposition on a substrate held at 200–500 °C has large perpendicular magnetic anisotropy.<sup>1–6</sup> The bulk equilibrium phase of this material has either *L1*<sub>0</sub> symmetry or a disordered face-centered-cubic (fcc) structure,<sup>7</sup> so uniaxial anisotropy is unexpected; in fact, when the samples are annealed at high temperatures, bulk phases form and the anisotropy disappears.<sup>4</sup> Thus, the anisotropy is created during growth. Experimental evidence suggests that clusters of Co form on the growth surface and are buried under subsequently arriving material.<sup>4–6</sup> Attempts by our group and by others to image these clusters directly with transmission electron microscopy and diffuse x-ray scattering have failed,<sup>5</sup> whereas extended x-ray absorption fine structure (EXAFS) spectroscopy shows increased Co–Co coordination in the film plane compared with the normal direction.<sup>8,9</sup>

In previous studies only deposition on flat substrates, terminated along the (100), (111) or (110) planes have been dealt with.<sup>5</sup> In this letter we discuss the effect of depositing on a vicinal substrate, miscut at a small angle toward the (100) direction. This miscut introduces steps on the growth surface, and the small step size should affect the formation of Co platelets, at least in the early stages of growth.

All samples were grown in an ultrahigh vacuum (UHV) e-beam evaporation chamber, with a base pressure of  $5 \times 10^{-10}$  Torr and a deposition pressure of  $5 \times 10^{-9}$  Torr. The substrates used were MgO (100) miscut by 2°, 4°, and 10°, corresponding to an average step size of 29, 14 and 6 lattice spacings, respectively. In addition one nonmiscut substrate was included as a control. CoPt<sub>3</sub> has a fcc structure, similar to a MgO substrate, although with a 10% mismatch in lattice parameter (3.83 Å for CoPt<sub>3</sub> versus 4.21 Å for MgO). During each run we deposited on a full representative set of substrates simultaneously, so the composition is the same for all miscut angles. The deposition rate for all samples was 0.5 Å/s, to a final thickness of 300 Å.

The samples were intentionally kept thin to ensure that the surface morphology would not change much, and thus effects from the surface steps remain important throughout the deposition. The substrate temperature was held constant during deposition at 400 °C. Previous work<sup>4</sup> showed that the perpendicular anisotropy is strongly dependent on the substrate temperature during growth, and has a peak at a deposition temperature of 400 °C. Above 450 °C, bulk mobility takes over and destroys the effect, and below 200 °C the surface mobility is too low for the Co clusters to form on the surface.

CoPt<sub>3</sub> samples grow epitaxially with a (100) orientation on (100)-oriented MgO substrates, which are cleaned before deposition by heating in vacuum to 450 °C for 30 min. Pre-annealing the MgO substrates to high temperatures (>750 °C) before the deposition had the unexpected result of creating a (111) growth direction of the films. The reflection high-energy electron diffraction (RHEED) patterns observed for this set of samples indicates a twinned epitaxial growth and not simple (111) texturing. Both the epitaxial (100) and twinned (111)-oriented films were included in the study for comparison. The crystallographic orientation of the single-crystal samples was characterized using a high-resolution x-ray diffractometer. The rocking-curve width of the (200) sample peak in the (100)-oriented samples is 1.1°, and the width of the (111) line in the twinned samples is 1.6°. A (311) line at the expected location in *k* space (no rotational symmetry) confirms the heteroepitaxial nature of these samples.

A vibrating sample magnetometer (VSM) was used to measure the hysteresis loops of the samples at room temperature. The saturation magnetization ( $M_S$ ) is independent of the miscut angle to within instrumental error. Small pieces of the samples were annealed under UHV conditions at temperatures >700 °C to drive them into the fcc chemically disordered state, where their magnetic properties are a known function of the composition. Magnetic analysis of the samples after annealing shows that the actual composition of the samples is 22% Co in the 400 °C epitaxial (100)-oriented

<sup>a)</sup>Electronic mail: bbm@physics.ucsd.edu

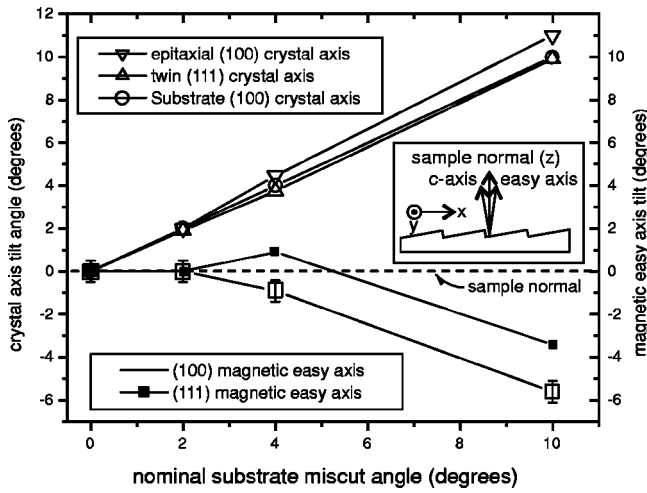


FIG. 1. Angle of crystallographic axes (sample and substrate) and magnetic easy axis (sample) measured with respect to the normal to the surface. Upper points are crystal tilts, lower points are magnetic easy axis tilts. The inset is a diagram of the side view of a 10° miscut sample that indicates the relevant axes.

samples, and 23% Co in the 400 °C twinned epitaxial (111)-oriented samples.

Figure 1 shows the relationship of the magnetic and structural axes to the surface normal. The crystal axis tilts were measured by a high-resolution x-ray diffraction (XRD) characterization of the samples to an accuracy greater than ±0.02°, showing that in all the (100) films, the *c* axis of the film is more tilted away from the surface normal than is the substrate *c* axis, with the difference becoming larger with a larger miscut angle. The (111) axes of the twinned samples, while well aligned with the substrate (100) axis, show a similar effect but instead are less tilted away from the surface normal than the substrate (100) axis, with the difference again growing larger at larger miscut angles. This tilting is explained by previous work on other systems, in which strain relaxation of epitaxial films grown on vicinal substrates is shown to occur through additional tilting of the growing sample.<sup>10,11</sup> The twinned (111) sample is expected to have small grains and thus has more nucleation centers for strain-relieving defects.

The magnitude of the perpendicular magnetic anisotropy of our samples was determined at room temperature with a torque magnetometer. For this measurement, we define  $\hat{z}$  as the surface normal direction,  $\hat{y}$  as the direction in-plane parallel to the vicinal step edges and  $\hat{x}$  as the in-plane direction perpendicular to the step edges. Scans were taken in the  $\hat{x}-\hat{z}$  plane and the  $\hat{y}-\hat{z}$  plane. The curves in the  $\hat{y}-\hat{z}$  plane show twofold symmetry, indicative of simple uniaxial anisotropy, while the curves in the  $\hat{x}-\hat{z}$  plane are more complicated, and reflect the broken symmetry of the system. Representative examples of  $\hat{x}-\hat{z}$  and  $\hat{y}-\hat{z}$  scans are included as insets in Fig. 2. The energy required to rotate the magnetic moment from the  $\hat{z}$  axis to the  $\hat{x}$  and  $\hat{y}$  axes, which we will call  $K_{xz}$  and  $K_{yz}$ , respectively, is plotted in Fig. 2. The values are obtained by integrating the torque curves and then subtracting the contribution of the shape magnetic anisotropy to give the intrinsic anisotropy. The almost constant values of  $K_{yz}$  suggest that the anisotropy associated with platelet formation during growth is unaffected by the step size. The

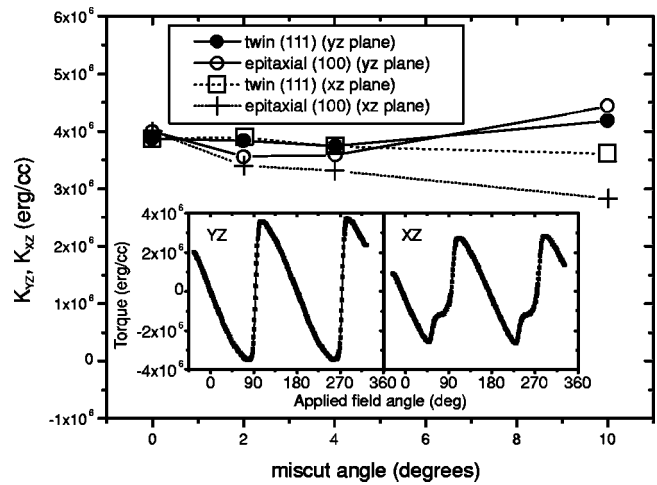


FIG. 2. Anisotropy energy, defined as the integral of torque curves from the easy ( $\hat{z}$ ) axis to the  $\hat{x}$  and  $\hat{y}$  axes. The inset is a plot of torque vs the angle of applied field relative to the surface normal for the 10° miscut (100) sample in the  $\hat{y}-\hat{z}$  and  $\hat{x}-\hat{z}$  planes. There is a small hysteresis between clockwise and counterclockwise rotations, not visible on this scale. Measurements were made at 2.1 T at room temperature.

small decrease in the magnitudes of  $K_{xz}$  with larger miscut angles suggests that additional anisotropy with an easy axis near  $\hat{x}$  in the  $\hat{x}-\hat{z}$  plane develops as the step density increases, consistent with the more complicated  $\hat{x}-\hat{z}$  torque curves.

The magnetic easy axis of our samples was also determined from the torque curves. The angle between the film easy axis (torque equals zero) and the film normal was determined to within ±0.1°, also plotted in Fig. 1. The direction of the vicinal tilt was defined to be positive for the plot. In all cases, the easy axis is found in the  $\hat{x}-\hat{z}$  plane. The easy axis of the 2° and 4° miscut samples is seen to be much closer to the surface normal than to the crystal *c* axis. The small tilting of the easy axis in a direction away from the miscut angle is consistent with the presence of two independent anisotropy components, one aligned with the surface normal and a much smaller one aligned with the width of the steps.

Figure 3(a) is a plot of the coercive field  $H_C$ , determined from the  $M(H)$  data, as a function of the miscut

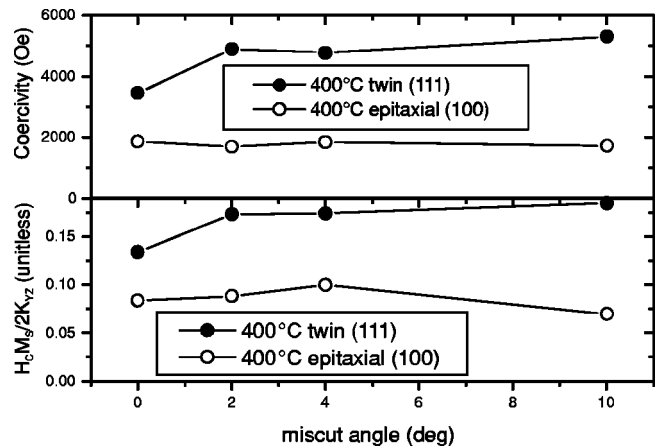


FIG. 3. (a) Coercive field, measured with  $H$  applied along the perpendicular (easy axis) direction. (b) Normalized coercivity  $H_C M_s / 2K_{yz}$ , the ratio between the measured magnetic reversal energy and the expected coherent rotation energy from the anisotropy.

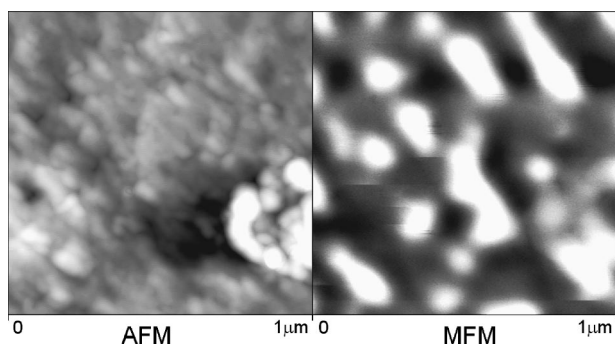


FIG. 4. Atomic and magnetic force microscopy images of the  $10^\circ$  miscut (100) sample. Both panels cover the same region of the sample. Vicinal steps are aligned along the  $45^\circ$  angle from upper left to lower right, and their effect on the epitaxial  $\text{CoPt}_3$  structure is visible in the AFM image. The full scale of AFM from white to black is  $200 \text{ \AA}$ , with an average surface roughness of  $28 \text{ \AA}$ .

angle, while Fig. 3(b) is a plot of  $H_C M_S / 2K_{yz}$ , a dimensionless quantity which scales the reversal energy by the anisotropy energy. The twinned (111) samples have significantly higher coercivity, consistent with smaller grains and a higher density of pinning sites. The coercivities of the epitaxial (100) and the twinned (111) samples are virtually unaffected by the step density.

We have studied the (100) films with magnetic force microscopy (MFM) and atomic force microscopy (AFM). Figure 4 is an AFM/MFM scan of the  $10^\circ$  miscut (100) sample in the thermally demagnetized state. The panel on the left is the AFM and the panel on the right is the MFM. Both scans were taken over the same area of the sample. The AFM image shows faceting aligned along the vicinal steps, which are oriented roughly along a  $45^\circ$  line from the upper-left corner to the lower-right corner. The MFM image clearly shows pinning of domains along the length of the steps. The magnetic field of the MFM tip was strong enough to move the domains around, but after three scans, the domain structure stabilized, and this stable state is the one depicted in Fig. 4. The resultant striped domain pattern has large areas which are visibly aligned with the vicinal step edge. The direction of the vicinal steps was independently determined from the x-ray diffraction analysis.

We have also looked at epitaxial samples grown at  $250^\circ\text{C}$  on vicinal substrates. We have previously found that the anisotropy of samples grown at  $250^\circ\text{C}$  is significantly reduced compared with samples grown at  $400^\circ\text{C}$ , and de-

pends on the growth rate.<sup>5</sup> When grown at  $250^\circ\text{C}$  on the miscut substrates, we find that higher-order terms dominate the anisotropy, making it difficult to extract and interpret values for the easy axis direction and the anisotropy, but there is no systematic change in either quantity with the miscut angle.

In conclusion, we have shown that the miscut angle and the correspondingly small substrate step size have little effect on growth-induced perpendicular magnetic anisotropy. An additional, smaller, in-plane anisotropy develops with a larger tilt angle, causing tilting of the global easy axis in a direction opposite to the crystal tilt direction. This definitively shows that the anisotropy is not tied to the crystal structure, in agreement with previous results which show little difference in anisotropy among samples grown with a (100), (111) or (110) orientation. Domain wall pinning was seen to occur parallel to vicinal step edges, although the miscut angle does not seem to significantly affect reversal energy. The faceting seen in the AFM images may produce locally flat growth surfaces, ones much larger than the average step size.

Thanks to the U.S. DOE for financial support of this work (Grant No. DE-FG03-95ER45529). Two of the authors (D.M.S. and E.T.Y.) would like to acknowledge financial support by the National Science Foundation (Grant No. DMR-0072912).

<sup>1</sup>C. J. Lin and G. Gorman, Appl. Phys. Lett. **61**, 1600 (1992).

<sup>2</sup>D. Weller, H. Brandle, G. Gorman, C.-J. Lin, and H. Notarys, Appl. Phys. Lett. **61**, 2726 (1992).

<sup>3</sup>D. Weller, H. Brandle, and C. Chappert, J. Magn. Magn. Mater. **121**, 461 (1993).

<sup>4</sup>P. W. Rooney, A. L. Shapiro, M. Q. Tran, and F. Hellman, Phys. Rev. Lett. **75**, 1843 (1995).

<sup>5</sup>A. L. Shapiro, P. W. Rooney, M. Q. Tran, F. Hellman, K. M. Ring, K. L. Kavanagh, B. Rellinghaus, and D. Weller, Phys. Rev. B **60**, R12826 (1999).

<sup>6</sup>M. Maret, M. C. Cadeville, R. Poinso, A. Herr, E. Beaurepaire, and C. Monier, J. Magn. Magn. Mater. **166**, 45 (1997).

<sup>7</sup>M. Hansen and K. Anderko, *Constitution of Binary Alloys* (McGraw-Hill, New York, 1986), p. 492.

<sup>8</sup>T. A. Tyson, S. D. Conradson, R. F. C. Farrow, and B. A. Jones, Phys. Rev. B **54**, 3702 (1996).

<sup>9</sup>C. Meneghini, M. Maret, M. C. Cadeville, and J. L. Hazemann, J. Phys. IV **7**, C2-1115 (1997); C. Meneghini, M. Maret, V. Parasote, M. C. Cadeville, J. L. Hazemann, R. Cortes, and S. Colonna, Eur. Phys. J. B **7**, 347 (1999).

<sup>10</sup>H. Nagai, J. Appl. Phys. **45**, 3789 (1974).

<sup>11</sup>F. Riesz, J. Vac. Sci. Technol. A **14**, 425 (1996).